Aurophilic Attraction and Luminescence of Binuclear Gold(I) Complexes with Bridging Phosphine Ligands: ab initio Study

Hong-Xing Zhang and Chi-Ming Che*[a]

Abstract: Electronic structure and spectroscopic properties of $[Au_2(dpm)_2]^{2+}$ (dpm = bis(diphosphino)methane) were studied by ab initio calculations. The absorption and emission spectra of this binuclear gold(I) complex in acetonitrile and in the solid state were calculated by single excitation configuration interaction (CIS) method. In the calculations, the solvent effect was taken into account by the weakly solvated $[Au_2(dpm)_2]^{2+}\cdot(MeCN)_2$ complex. The ground state structures of $[Au_2(dpm)_2]^{2+}$ and $[Au_2(dpm)_2]^{2+}\cdot(MeCN)_2$ were optimized by the second-order Møller–Plesset perturbation (MP2) method, while the emissive triplet excited state structures were optimized by the CIS calculations. The results reveal that coordination of acetonitrile to the gold atom in the $^3[d_{\sigma^*}s_\sigma]$ excited state causes a significant red shift in emission energy. The weak aurophilic attraction exists in the ground states of $[Au_2(dpm)_2]^{2+}$ and $[Au_2(dpm)_2]^{2+}\cdot(MeCN)_2$, and is greatly enhanced in their $^3[d_{\sigma^*}s_\sigma]$ excited states. In acetonitrile, the $^3A_u(s_\sigma) \rightarrow {}^1A_g(d_{\sigma^*})$ transition (phosphorescence) of $[Au_2(dpm)_2]^{2+}$ was calculated at 557 nm, in consistent with the observed emission of $[Au_2(dppm)_2](ClO_4)_2$ (dppm = bis(diphenylphosphino)methane) at 575 nm. A high energy emission at 331 nm is predicted for $[Au_2(dpm)_2]^{2+}$ in the absence of the interaction between the gold atom and solvent molecule and/or neighboring anion in the excited state. The CIS calculations on the excited states also reveal that the two absorption bands at 278 and 218 nm recorded for $[Au_2(dcpm)_2](ClO_4)_2$ in acetonitrile can be attributed to the $^1A_g(d_{\sigma^*}) \rightarrow {}^1A_u(p_\sigma)$ and $^1A_g(d_{\sigma^*}) \rightarrow {}^1A_u((sp)_\sigma)$ transitions, respectively.

Keywords: ab initio calculations · aurophilic interaction · gold · luminescence · solvent effects

Introduction

The aurophilic attraction[1–4] and photoluminescence[5–12] of gold(I) complexes have kept gold(I) chemistry to be one of the most attractive fields in recent years. A wide range of luminescent gold(I) complexes have been synthesized and structurally characterized, and their absorption and emission spectra have been examined in considerable detail.[3, 5–10] Very precise computations, taking electron correlation and relativistic effects into account, have estimated the strength of weak Au^I-Au^I interaction.[1, 2, 4] In addition, theoretical Xα, and SCF calculations have been undertaken to rationalize the luminescent properties of gold(I) complexes.[5] In light of the difference in absorption and emission properties between mononuclear and binuclear gold(I) phosphine complexes, the relationship between aurophilic attraction (intra- and intermolecular) and luminescence behavior has been emphasized.[5–7, 9–13] The lowest energy emissions of binuclear gold(I) complexes containing bridging phosphine ligands have previously been assigned to metal-localized transitions, and aurophilic attraction was involved to explain the red shift in photoluminescence from the mononuclear to binuclear complexes. For example, the 575 nm emission of $[Au_2(dppm)_2][ClO_4]_2$ (dppm = bis(diphenylphosphino)methane) recorded in acetonitrile was attributed to the metal-localized $6p_\sigma \rightarrow 5d_{\sigma^*}$ transition.[5, 6] For (TPA)AuSPh (TPA = 1,3,5,-triaza-7-phosphaadamantanetriylphosphine) and its derivatives, their lowest energy emissions were attributed to ligand-to-metal charge transfer (LMCT) transitions.[10]

In principle, no bonding interaction is to be expected between two closed-shell metal ions with an $nd^{10}(n+1)s^0$ electronic configuration. However, results from extensive experimental and theoretical studies revealed that a weak bonding exists between two gold(I) atoms at a separation of less than 3.5 Å.[1, 2] Indeed, there are many gold(I) complexes (such as $[Au_2(dppm)_2]^{2+}$,[5, 6] $Au_2X_2(dppm)$ (X = Cl, Br, and I),[3, 14] and $AuCl(PPh_3)$[15]) that show intra- and intermolecular weak Au^I-Au^I bonding attraction with stabilization energy estimated to be around 5–10 kcal mol^{-1}.[1–3] In these gold(I) phosphine complexes, the phosphine ligands are electron donors which would partially neutralize the positive charge localized on the gold atoms through the Au–P dative

[a] Prof. C.-M. Che, Prof. H.-X. Zhang
Department of Chemistry
The University of Hong Kong
Pokfulam Road (Hong Kong)
Fax: (+852) 2857-1586
E-mail: cmche@hkucc.hku.hk

  0947-6539/01/0722-4887 $ 17.50+.50/0

bonding interactions. This leads to partial electronic charge to reside on the 6s and 6p orbitals of Au^I and results in a breakdown of the closed-shell $5d^{10}6s^0$ configuration, thus accounting for the aurophilic attraction. Pyykkö and co-workers also attributed the aurophilic attraction to relativistic effect together with dispersive interaction.[2, 16]

Although gold(I) is usually two-coordinated with a linear coordination geometry, three-coordinated gold(I) species are not uncommon.[8, 17] In two-coordinate cationic gold(I) phosphine complexes such as $[Au_2(dppm)_2]^{2+}$, $[Au_2(dcpm)_2]^{2+}$ (dcpm = bis(dicyclohexylphosphino)methane),[18] and $[Au_2(dmpm)_2]^{2+}$ (dmpm = bis(dimethylphosphino)methane),[19] the gold atoms bear positive electronic charge. Therefore, upon dissolution of these species in acetonitrile, the three-coordinated weakly solvated gold(I) complexes as shown in Equation (1) are likely to exist. Indeed, X-ray crystal structure of $[Au_2(dmpm)_2]Cl_2$ revealed that the AuP_2 moieties weakly interact with the Cl^- anions with the Au–Cl distances being 3.49(2) Å.[19a] Consequently, we envisaged that the emission and absorption properties of two-coordinate gold(I) phosphine complexes would be affected by solvent and/or neighboring nucleophilic molecules.

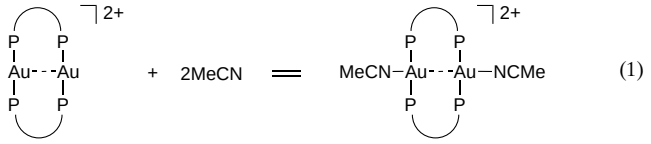

(1)

In the literature, there are many examples of binuclear gold(I) phosphine complexes which show visible photoluminescence in solution, the emission maxima of which are dramatically red-shifted from the lowest energy dipole-allowed electronic transitions of these complexes.[12] For example, the lowest energy dipole-allowed transition of $[Au_2(dppm)_2](ClO_4)_2$ is at 292 nm, but the emission maximum of this complex recorded in acetonitrile is at 575 nm.[5, 6] Such a large Stokes shift (2.09 eV) between the absorption and emission energies is very striking and demands a better understanding of the nature of the excited states. In this work, we employed ab initio methods to study the electronic structure and spectroscopic properties of the $[Au_2(dpm)_2]^{2+}$ (dpm = bis(diphosphino)methane) and the weakly solvated $[Au_2(dpm)_2]^{2+}\cdot(MeCN)_2$ cations. The calculations indicate that coordination of acetonitrile to the gold atoms in the excited state is primarily responsible for the visible emission spectra. The weak aurophilic attraction exists in the ground states of $[Au_2(dpm)_2]^{2+}$ and $[Au_2(dpm)_2]^{2+}\cdot(MeCN)_2$, and is greatly enhanced in their $^3(d_{\sigma^*}s_\sigma)$ excited states. A high energy emission at 331 nm is predicted for the $[Au_2(dpm)_2]^{2+}$ cation when the solvent and anion interaction with the gold atoms in the excited state is absent.

Computational details

In this work, $[Au_2(dpm)_2]^{2+}$ was used as a computational model for $[Au_2(dppm)_2]^{2+}$, $[Au_2(dcpm)_2]^{2+}$, and $[Au_2(dmpm)_2]^{2+}$. The same model compound had previously been employed by Fackler and co-workers in their SCF-Xα-SW molecular orbital study on the photoluminescence of $[Au_2(dppm)_2](BF_4)_2$.[5] In fact, it is not uncommon in ab initio calculations to use hydrogen to substitute phenyl, methyl, or cyclohexyl groups in phosphine ligands. Pyykkö and Schmidbaur have also adopted this approach in their theoretical studies on the aurophilic attraction in mononuclear and polynuclear gold(I) phosphine complexes.[16] Härberlen and Rösch have investigated the effect of phosphine substituents in gold(I) complexes by the linear combination of Gaussian-type orbitals (LCGTO) local density functional (DFT) method to obtain the optimized Au–P bond lengths of 2.29, 2.25, and 2.28 Å for $MeAuPH_3$, $MeAuPMe_3$, and $MeAuPPh_3$ respectively.[16c]

To account for the solvent effect on the spectroscopic properties, two acetonitrile molecules were added to the gold atoms as depicted in Figure 1 to give a quasi three-coordinated $[Au_2(dpm)_2]^{2+}\cdot(MeCN)_2$ complexes. This supposition is not unrealistic as there are a number of three-coordinate gold(I) complexes with T-shape structures in the literature.[17b, 19] Figure 1 also presents the structure of the $[Au_2(dpm)_2]^{2+}$ cation.

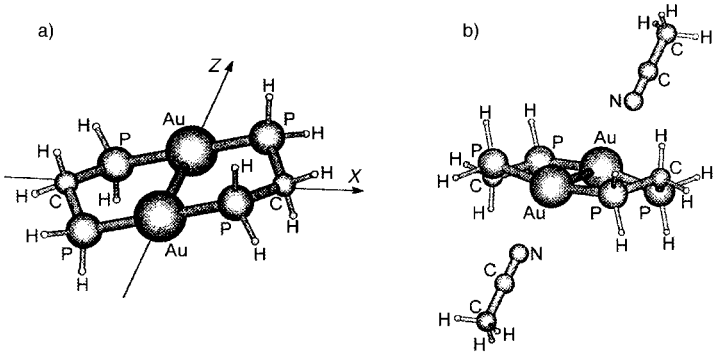

Figure 1. The optimized structure of the ^1A_g ground state of a) $[Au_2(dpm)_2]^{2+}$ and b) $[Au_2(dpm)_2]^{2+}\cdot(MeCN)_2$ using MP2 calculations.

The second-order Møller–Plesset (MP2) method[20] has widely been used for ground state calculations[21] and the configuration interaction (CI) method[22] is one of the best methods for the excited state calculations.[23] Full optimizations on the ground state structures were performed under the MP2 calculations for both $[Au_2(dpm)_2]^{2+}$ and $[Au_2(dpm)_2]^{2+}\cdot(MeCN)_2$. Based on these calculations, single excitation configuration interaction (CIS) calculations were carried out to reveal the excited state electronic structures. In the calculation of emission spectrum, the excited structure was fully optimized.

In the calculations, quasi-relativistic pseudopotentials of the Au and P atoms proposed by Hay and Wadt[24] with 19 and 5 valence electrons, respectively, were employed and the LANL2DZ basis sets associated with the pseudopotential were adopted. The basis sets were taken as Au(8s6p4d/3s3p2d), P(3s3p/2s2p), N(10s5p/3s2p), C(10s5p/3s2p), and H(4s/2s). Thus, 118 basis functions and 80 electrons for $[Au_2(dpm)_2]^{2+}$, and 184 basis functions and 134 electrons for $[Au_2(dpm)_2]^{2+}\cdot(MeCN)_2$ were included in the calculations. All the calculations were accomplished using the Gaussian 94 program package[25] and on a Silicon Graphics Indigo 2 workstation.

0947-6539/01/0722-4888 $ 17.50+.50/0 *Chem. Eur. J.* **2001**, *7*, No. 22

The basis set is an important parameter in ab initio calculations. In general, a larger basis set can lead to a more accurate calculation, but would demand more computational time and recourses, especially in investigations of the excited state. We have examined the impact of the phosphorous 3d orbitals in our computational models by performing calculations on the $[Au(PH_3)_2]^+$ monomer. Table 1 shows the optimized structures of the ground state (by MP2 method) and the excited state (by CIS method) for $[Au(PH_3)_2]^+$ with and without a phosphorous d function in the calculation. The result indicates that the P 3d orbitals have only a very little effect on the ground and excited states. Therefore, we did not incorporate such orbitals in our chosen basis set for the subsequent calculations to save computational time.

Table 1. The optimized structures of $[Au(PH_3)_2]^+$ in the ground and excited state under the MP2 and CIS calculations.

Parameter	Ground state $^1A_{1g}$		Excited state $^3A_{2u}$	
	without d function	with 1 d function	without d function	with 1 d function
Au–P [Å]	2.448	2.444	2.875	2.886
P–H [Å]	1.417	1.418	1.408	1.409
Au-P-H [°]	115.07	115.11	116.00	116.05

In their crystalline forms, the $[Au_2(dppm)_2]^{2+}$,[5, 6] $[Au_2(dcpm)_2]^{2+}$,[18] and $[Au_2(dmpm)_2]^{2+}$[19] complexes have a chair conformation with a C_i symmetry. For this reason, the model complex, $[Au_2(dpm)_2]^{2+}$, was also set to have a C_i symmetry as depicted in Figure 1. This is different from previous works where C_{2h} symmetry for the same model complex,[5] with all the Au and P atoms being coplanar, was adopted in the calculations. For $[Au_2(dpm)_2]^{2+}$, there is only a slight difference between the C_i and C_{2h} structures. However, as discussed in later sections, when the solvent molecules are taken into account, the assignment of C_{2h} symmetry is not appropriate, because the Au and P atoms are no longer co-planar.

Under the C_i symmetry and the basis sets employed, the total 118 orbitals of $[Au_2(dpm)_2]^{2+}$ are reduced to 59 a_g and 59 a_u irreducible orbitals. Likewise, the 184 orbitals of $[Au_2(dpm)_2]^{2+}\cdot(MeCN)_2$ are reduced to 92 a_g and 92 a_u irreducible orbitals. All these orbitals were included in the MP2 and CIS calculations in order to have all of the possible electron correlations in the present computational level. To facilitate the post-calculation treatment, for both $[Au_2(dpm)_2]^{2+}$ and $[Au_2(dpm)_2]^{2+}\cdot(MeCN)_2$, the origin was put in the middle of the two Au atoms, and the z axis orients to an Au atom, while the x axis points to the bridging C atom of the dpm moiety (Figure 1).

Results and Discussion

In recent years, extensive studies have been performed on the photoluminescence and photophysical properties of binuclear and polynuclear gold(i) complexes.[12] With the aid of semi-empirical quantum chemical calculations, the absorption and emission spectra of some gold(i) complexes have been assigned. By SCF-Xα-SW calculation, Fackler and co-workers assigned the 292 nm absorption and low energy emission of $[Au_2(dppm)_2]^{2+}$ in acetonitrile to the respective spin-allowed $\sigma^*(s,d_{z^2}) \rightarrow \sigma(p_z)$ and spin-forbidden $\sigma(p_z) \rightarrow \sigma^*(s,d_{z^2})$ ($^3A_u \rightarrow {}^1A_g$) transitions under a C_{2h} symmetry.[5] We gave the same assignment to the 292 nm absorption band and proposed the lowest triplet emissive state to be $(d_{\delta^*})^1(p_\sigma)^1$ in nature.[6] In this work ab inito calculations on the excited states of $[Au_2(dpm)_2]^{2+}$ and $[Au_2(dpm)_2]^{2+}\cdot(MeCN)_2$ were performed, in order to address the large Stokes shift of the 292 nm absorption band and the low energy emission of $[Au_2(dppm)_2]Y_2$ at 575 ($Y = ClO_4$)[6] and 593 nm ($Y = BF_4$)[5] measured in acetonitrile.

The full MP2 optimization on the $[Au_2(dpm)_2]^{2+}$ and $[Au_2(dpm)_2]^{2+}\cdot(MeCN)_2$ cations indicated that the former has a ^1A_g ground state either in the solid state or in acetonitrile. The main optimized geometrical parameters are listed in Table 2. In $[Au_2(dpm)_2]^{2+}$, the Au^I adopts a linear two-coordinate geometry. The dihedral P-Au-Au-P angle and P-Au-P angle are 179.3° and 179.4°, respectively; this suggests that the Au and P atoms are almost co-planar. However, in $[Au_2(dpm)_2]^{2+}\cdot(MeCN)_2$, these two angles change into 166.9° and 167.2°, respectively. This reveals that the interaction between Au^I and the acetonitrile molecule pulls the former out of the plane spanned by the Au and P atoms in opposite direction. Therefore, the C_{2h} symmetry is only valid for $[Au_2(dpm)_2]^{2+}$, but not for $[Au_2(dpm)_2]^{2+}\cdot(MeCN)_2$. For $[Au_2(dpm)_2]^{2+}\cdot(MeCN)_2$, the calculated Au–N(MeCN) distances are 2.583 Å, which indicates that the MeCN molecule is weakly bonded to Au^I in the ground state. The Au–Au bond lengths are 3.167 and 3.155 Å for $[Au_2(dpm)_2]^{2+}$ and $[Au_2(dpm)_2]^{2+}\cdot(MeCN)_2$, respectively. This points to the existence of a weak Au–Au attraction. Very recently, Pyykkö and co-worker optimized the ground state structure of $[Au_2(dpm)_2]^{2+}$ by adding one d function and one f function for the P and Au atoms into the LANL2DZ basis set.[2c] They

Table 2. The main geometry parameters of the ^1A_g ground state for $[Au_2(dpm)_2]^{2+}$ and $[Au_2(dpm)_2]^{2+}\cdot(MeCN)_2$ under the MP2 calculations.

Parameter	$[Au_2(dpm)_2]^{2+}$	$[Au_2(dpm)_2]^{2+}\cdot(MeCN)_2$
bond length [Å]		
Au–Au	3.167	3.155
Au–P	2.451	2.448
C–P	1.905	1.903
Au–N		2.583
N–C		1.203
C–C		1.489
bond angle [°]		
P-C-P	114.0	112.3
P-Au-P	179.4	167.2
P-Au-Au	90.3	91.6
C-P-Au	113.3	114.0
Au-Au-N		117.2
dihedral angle [°]		
P-Au-Au-P	179.3	166.9

obtained equilibrium Au–Au and Au–P bond lengths of 2.969 and 2.341 Å, respectively, which implies the f function of Au shortens the Au–Au and Au–P bond lengths. We have not included f functions of Au in our calculations after considering the optimization capacity of the Gaussian 94 program package in second derivatives of f basis under core potential techniques. On the other hand, the difference of the Au–Au bond lengths arising from the f function may not be very significant as it is a weak interaction.

The MP2 calculation on $[Au_2(dpm)_2]^{2+}$ shows that the Au atoms have a net +0.10 positive electronic charge, while the electronic charge residing on the P atoms is +0.53. This is in line with the expected charge transfer from the P lone pair to the empty 6s and 6p orbitals of Au^I. Consequently, the positive charge of the gold atom is partially neutralized and the closed-shell $5d^{10}6s^0$ electronic configuration is no longer valid.

Based on the ground state structure of $[Au_2(dpm)_2]^{2+}\cdot(MeCN)_2$, we performed the CIS calculation with an objective to evaluate the electronic structure of its excited states obtained by direct electronic excitation in acetonitrile. The three calculated allowed transitions are listed in Table 3 together with the spectroscopic data of $[Au_2(dppm)_2](ClO_4)_2$ and $[Au_2(dcpm)_2](ClO_4)_2$ recorded in acetonitrile for comparison.

Table 3. The calculated absorptions of $[Au_2(dpm)_2]^{2+}\cdot(MeCN)_2$ at the CIS level as compared with the observed absorptions of $[Au_2(dcpm)_2](ClO_4)_2$ (ref. [18]) and $[Au_2(dppm)_2](ClO_4)_2$ (refs. [5] and [6]) in acetonitrile.

transition	$[Au_2(dpm)_2]^{2+}\cdot(MeCN)_2$ λ_{calcd} [nm]	oscillator strength	$[Au_2(dcpm)_2](ClO_4)_2$ λ [nm]	$[Au_2(dppm)_2](ClO_4)_2$ λ [nm]
$X^1A_g \rightarrow A^1A_u$	245.7	0.284	278	292
$X^1A_g \rightarrow B^1A_u$	227.4	0.002	243	
$X^1A_g \rightarrow C^1A_u$	215.6	0.155	218	

Because of the C_i symmetry of $[Au_2(dpm)_2]^{2+}\cdot(MeCN)_2$ and its ground state of ^1A_g, for dipole allowed transition, the excited state should have a ^1A_u symmetry. Table 4 gives the gross orbital population of each atom in $[Au_2(dpm)_2]^{2+}\cdot(MeCN)_2$ for the ^1A_g ground state and the three low-lying ^1A_u excited states.

We can see that the population on the dpm ligands and the MeCN molecules for the A^1A_u and C^1A_u excited states is almost the same as that of the X^1A_g ground state, implying that only charge transfer within the Au atoms is involved in the $X^1A_g \rightarrow A^1A_u$ and $X^1A_g \rightarrow C^1A_u$ transitions. In the X^1A_g ground state, the electronic configuration of the Au atom is $5d^{9.876}6s^{0.647}6p^{0.387}$, while in the A^1A_u, B^1A_u, and C^1A_u excited states the configurations are $5d^{9.622}6s^{0.690}6p^{0.609}$, $5d^{9.875}6s^{0.648}6p^{0.392}$, and $5d^{9.613}6s^{0.784}6p^{0.525}$, respectively. The $X^1A_g \rightarrow A^1A_u$ transition calculated at 245.7 nm has the largest oscillator strength of 0.284; we relate this to the 278 nm band of $[Au_2(dcpm)_2](ClO_4)_2$[18] and the 292 nm band of $[Au_2(dppm)_2](ClO_4)_2$ recorded in acetonitrile.[5, 6] In this $X^1A_g \rightarrow A^1A_u$ transition about 0.26 5d electron of Au^I is transferred to the 6s and 6p orbitals at ratio 1:5 statistically. This results in a conventional $d_{\sigma^*} \rightarrow p_\sigma$ transition which we can intuitively understand from the density diagrams of the frontier orbitals as shown in Figure 2. In the $X^1A_g \rightarrow B^1A_u$ transition, the population of the atoms in the $[Au_2(dpm)_2]^{2+}$ moiety remains the same between the ground and excited states. Instead, the population on the CN group of acetonitrile differs as illustrated by the data listed in Table 4. This reveals that the transition does not originate from the $[Au_2(dpm)_2]^{2+}$ species but is due to acetonitrile. The third $X^1A_g \rightarrow C^1A_u$ transition is metal-localized and is assigned to be $d_{\sigma^*} \rightarrow (sp)_\sigma$ in nature, where $(sp)_\sigma$ denotes a σ-bonding orbital with a mixed s and p orbital character.

To describe the phosphorescence of $[Au_2(dpm)_2]^{2+}$ in solution and in the solid state, we optimized the structure of

Table 4. The gross orbital populations for the ground ^1A_g and three low-lying ^1A_u excited states of $[Au_2(dpm)_2]^{2+}\cdot(MeCN)_2$ involved in the electronic excitation.

	Atom	Orbital	^1A_g	^1A_u	^1A_u	^1A_u
$[Au_2(dpm)_2]^{2+}$	Au	6s	0.647	0.690	0.648	0.784
		6p	0.387	0.609	0.392	0.525
		5d	9.876	9.622	9.875	9.613
	C	2s	1.601	1.592	1.601	1.604
		2p	3.264	3.263	3.264	3.290
	P	3s	1.593	1.587	1.593	1.597
		3p	3.002	3.002	3.002	2.988
	H_C	1s	0.702	0.704	0.702	0.701
	H_C	1s	0.681	0.681	0.681	0.685
	H_P	1s	0.924	0.930	0.924	0.920
	H_P	1s	0.950	0.951	0.950	0.954
$(MeCN)_2$	N	2s	1.665	1.660	1.665	1.657
		2p	3.509	3.504	3.408	3.499
	C_N	2s	1.197	1.196	1.197	1.196
		2p	2.743	2.744	2.836	2.744
	C_H	2s	1.471	1.471	1.471	1.471
		2p	3.087	3.087	3.082	3.087

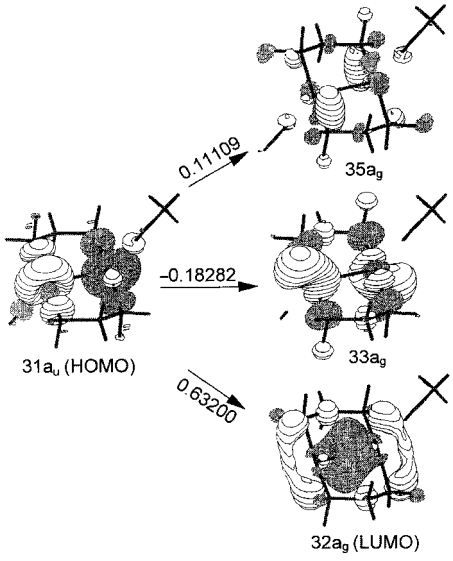

Figure 2. The single electron transitions with |CI coefficient| >0.1 in the CIS calculation for the 245.7 nm absorption of $[Au_2(dpm)_2]^{2+}\cdot(MeCN)_2$.

0947-6539/01/0722-4890 $ 17.50+.50/0 *Chem. Eur. J.* **2001**, *7*, No. 22

the first ^3A_u excited state for $[Au_2(dpm)_2]^{2+}$ and $[Au_2(dpm)_2]^{2+}\cdot(MeCN)_2$ by the CIS method. The optimized structures are shown in Figure 3, and the corresponding geometry parameters are listed in Table 5.

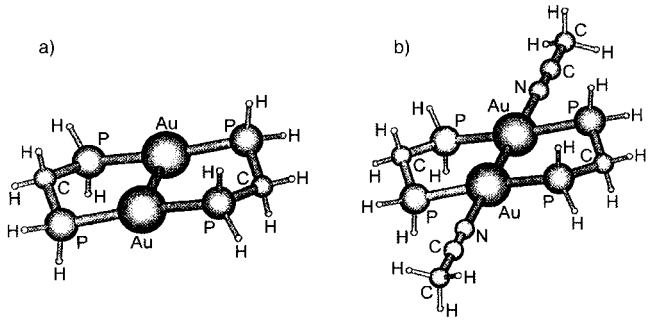

Figure 3. The optimized structure for the ^3A_u emissive state of a) $[Au_2(dpm)_2]^{2+}$ and b) $[Au_2(dpm)_2]^{2+}\cdot(MeCN)_2$ using the CIS calculations.

Table 5. The main optimized geometry parameters of the ^3A_u excited state for $[Au_2(dpm)_2]^{2+}$ and $[Au_2(dpm)_2]^{2+}\cdot(MeCN)_2$ under the CIS calculations.

Parameter	$[Au_2(dpm)_2]^{2+}$	$[Au_2(dpm)_2]^{2+}\cdot(MeCN)_2$
bond length [Å]		
Au–Au	2.745	2.719
Au–P	2.669	2.776
C–P	1.888	1.883
Au–N		2.377
N–C		1.147
C–C		1.470
bond angle [°]		
P-C-P	114.6	111.4
P-Au-P	170.9	171.8
P-Au-Au	94.5	94.1
C-P-Au	108.6	110.6
Au-Au-N		179.9

In the ^3A_u excited states of both cations, the Au and P atoms are co-planar. The shorter Au–Au bond length in the ^3A_u state of $[Au_2(dpm)_2]^{2+}\cdot(MeCN)_2$ compared with that of $[Au_2(dpm)_2]^{2+}$ implies that the Au–Au interaction in the ^3A_u excited state is slightly enhanced through coordination of MeCN to the gold atoms. The N and C atoms of the two acetonitrile molecules become co-planar with the Au and P atoms. In contrast to its ground state structure, the MeCN in the ^3A_u excited state of $[Au_2(dpm)_2]^{2+}\cdot(MeCN)_2$ is bonded to the Au atom with the calculated Au–N(MeCN) bond length of 2.377 Å. Furthermore, the Au–Au bond length of 2.719 Å reflects the formation of a Au–Au single bond. Indeed, the structure of the ^3A_u excited state of $[Au_2(dpm)_2]^{2+}\cdot(MeCN)_2$ resembles that of binuclear d^9-d^9 metal–metal bonded complexes. For example, the $[Au(CH_2)_2PPh_2]_2X_2$ and $[Au(CH_2)_2PPh_2]_2(CH_3)X$ (X = Cl, Br, and I) complexes are isostructural to the ^3A_u state of $[Au_2(dpm)_2]^{2+}\cdot(MeCN)_2$ with similar intramolecular gold–gold bond lengths [d(Au–Au) = 2.674(1) Å for $[Au(CH_2)_2PPh_2]_2(CH_3)Br$].[26] The formation of a Au–Au single bond in the ^3A_u state is consistent with the formulation of the electronic transition that involves promotion of an electron from a d_{σ^*} antibonding to s_σ bonding orbital. The Au–P bond lengths become longer, presumably as a result of the antibonding interaction between the s orbital of the Au atom and the p orbital of the P atom.

The calculated $^3A_u \rightarrow {}^1A_g$ transition (phosphorescence) of $[Au_2(dpm)_2]^{2+}\cdot(MeCN)_2$ is at 557 nm; this is consistent with the emission at 575 nm found for $[Au_2(dppm)_2](ClO_4)_2$ in acetonitrile at room temperature.[6] Table 6 shows the gross orbital population of the ^1A_g and ^3A_u states involved in this transition. By comparing the population between these two states as listed in Table 6, the emission could be attributed to

Table 6. The gross orbital populations for the ^1A_g and ^3A_u states of $[Au_2(dpm)_2]^{2+}\cdot(MeCN)_2$ involved in the 557 nm emission.

	Atom	Orbital	^1A_g	^3A_u
$[Au_2(dpm)_2]^{2+}$	Au	6s	0.472	0.726
		6p	0.323	0.398
		5d	9.919	9.631
	C	2s	1.600	1.598
		2p	3.315	3.313
	P	3s	1.628	1.625
		3p	3.009	2.997
	H_C	1s	0.700	0.700
	H_C	1s	0.678	0.679
	H_P	1s	0.947	0.951
	H_P	1s	0.971	0.972
$(MeCN)_2$	N	2s	1.596	1.587
		2p	3.526	3.518
	C_N	2s	1.213	1.212
		2p	2.762	2.761
	C_H	2s	1.461	1.461
		2p	3.107	3.107

electronic transition within the Au atoms. The electronic configuration of the Au atom is $5d^{9.919}6s^{0.472}6p^{0.323}$ and $5d^{9.631}6s^{0.726}6p^{0.398}$ in the ^1A_g ground state and ^3A_u excited state, respectively, which indicates that the 6s and 6p electrons transfer back to the 5d orbitals during the phosphorescence, and the 6s orbital plays a dominant role. The emission can be assigned to the $^3A_u(s_\sigma) \rightarrow {}^1A_g(d_{\sigma^*})$ transition, which can be well understood by analysing the single electron transition diagram in the CIS calculation as shown in Figure 4.

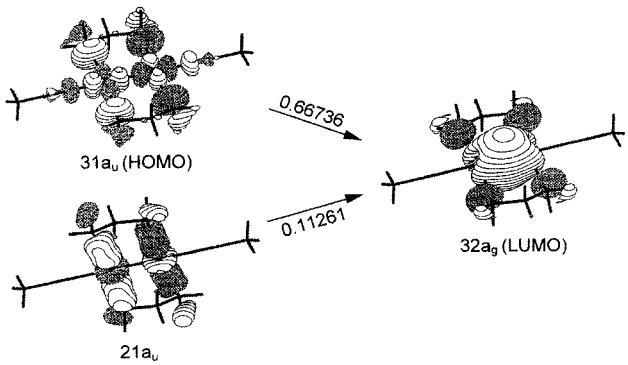

Figure 4. The single electron transitions with |CI coefficient| > 0.1 in the CIS calculation for the 557 nm emission of $[Au_2(dpm)_2]^{2+}\cdot(MeCN)_2$.

The orbital composition of the ^3A_u excited state responsible for the 557 nm emission is different from that of the ^1A_u excited state generated through direct electronic excitation at

245.7 nm. The ^1A_u excited state involves p_σ bonding of the two Au atoms, but s_σ bonding becomes important in the phosphorescent ^3A_u state. The origin of this difference is that the 6s orbital is lower in energy than the 6p orbitals. In the ^3A_u state, the shorter Au–Au separation of 2.719 Å enables the two Au 6s orbitals to overlap and form a σ bond. However, the polar 6p orbitals are more diffuse and hence only their overlapping is feasible at longer Au–Au separations. Therefore, when the Au–Au bond length is kept at 3.15 Å in the calculated $^1A_g \rightarrow {}^1A_u$ electronic excitation, the p_σ bonding becomes dominant in the ^1A_u excited state. Hence, the ^1A_u and ^3A_u states of $[Au_2(dpm)_2]^{2+} \cdot (MeCN)_2$ are designated to be p_σ and s_σ symmetry, respectively.

From the CIS calculations, we find that the $^3A_u \rightarrow {}^1A_g$ transition of the $[Au_2(dpm)_2]^{2+}$ cation is at 331 nm in the absence of solvent or anions. This could be the case of a $[Au_2(dpm)_2]^{2+}$ containing solid where the counteranions are distant apart from the gold atoms. The gross population listed in Table 7 shows that this transition is metal-localized. The

Table 7. The gross orbital populations for the ^1A_g and ^3A_u states of $[Au_2(dpm)_2]^{2+}$ involved in the 331 nm emission.

Atom	Orbital	^1A_g	^3A_u
Au	6s	0.637	0.789
	6p	0.316	0.408
	5d	9.909	9.648
C	2s	1.603	1.600
	2p	3.294	3.293
P	3s	1.604	1.607
	3p	2.997	2.998
H_c	1s	0.687	0.687
H_c	1s	0.661	0.661
H_p	1s	0.905	0.910
H_p	1s	0.941	0.942

electronic configuration of the Au atom is $5d^{9.909}6s^{0.637}6p^{0.316}$ and $5d^{9.648}6s^{0.789}6p^{0.408}$ for the respective ^1A_g and ^3A_u states of $[Au_2(dpm)_2]^{2+}$. This implies that partial 6s and 6p electron transfers to 5d orbital during the emission process at 331 nm. We assign the emission at 331 nm to the $^3A_u((sp)_\sigma) \rightarrow {}^1A_g(d_{\sigma^*})$ transition, as illustrated by the electronic transition diagrams depicted in Figure 5 in the CIS calculation. Note that the ^3A_u state of $[Au_2(dpm)_2]^{2+}$ has mixed s and p orbital characters and is denoted as $(sp)_\sigma$. Although high energy emission has not been reported for the $[Au_2(dppm)_2]Y_2$ solids ($Y = ClO_4$, BF_4),[5, 6] our recent study on $[Au_2(dcpm)_2](ClO_4)_2$[18] revealed the presence of an intense high energy solid state emission. The complex has an intramolecular Au–Au separation of 2.927 Å. At room temperature the complex displays an intense solid state emission at 368 nm, but the emission red-shifts to 510 nm upon dissolution in acetonitrile. The emission of $[Au_2(dcpm)_2](ClO_4)_2$ is assigned to the $\sigma \rightarrow \sigma^*$ transition where σ and σ* have a predominant s orbital and d orbital character, respectively.

In fact, the presence of anions near the $[Au_2(dpm)_2]^{2+}$ cation would affect the solid state emission. To test this proposition, $[Au_2(dpm)_2](ClO)_2$ was chosen as a model for $[Au_2(dpm)_2](ClO_4)_2$ in the CIS calculations. The ClO^- was

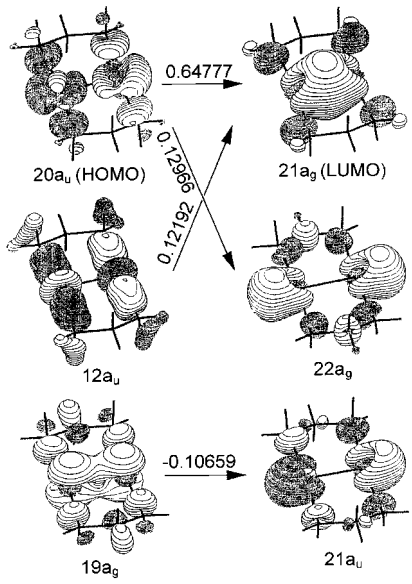

Figure 5. The single electron transitions with $|CI\ coefficient| > 0.1$ in the CIS calculation for the 331 nm emission of $[Au_2(dpm)_2]^{2+}$.

employed to replace ClO_4^- in order to save computational time. When the Au–OCl separation changes from 4.5 to 3.3 Å, and the C_i symmetry is kept, and the calculated emission wavelength varies from 356 to 406 nm. This result implies that the approach of the ClO^- anion to the Au atom causes a red shift in the emission spectrum.

If the interaction between the ClO^- anion and the $[Au_2(dpm)_2]^{2+}$ cation is electrostatic in nature, it is feasible that two negative background charges can be used to substitute the anion in the calculation. As shown in Figure 6,

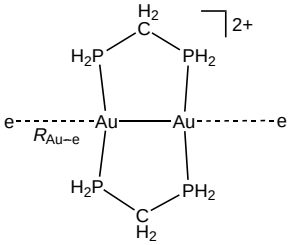

Figure 6. Diagrammatic representation of the interaction between the background charge and $[Au_2(dpm)_2]^{2+}$.

the two negative charges orient along the Au–Au axis, and the whole system composed of the negative charges and the $[Au_2(dpm)_2]^{2+}$ complex cation was kept the C_i symmetry.

Figure 7 shows the correlation between the calculated emission and the distance of the negative charge from the Au atom. As the distance changes from 8.0 to 3.0 Å, the emission energy red-shifts from 331 to 420 nm. This again reveals that the presence of neighboring anion would cause a red shift in the emission of the $[Au_2(dpm)_2]^{2+}$ moiety.

It is evident that the counteranion could have significant effect on the solid state emission of binuclear gold(I) phosphine complexes. This remains to be an interesting problem. We anticipate that for those gold(I) complexes with very bulky phosphine ligands, the counteranions will be

0947-6539/01/0722-4892 $ 17.50+.50/0 *Chem. Eur. J.* **2001**, *7*, No. 22

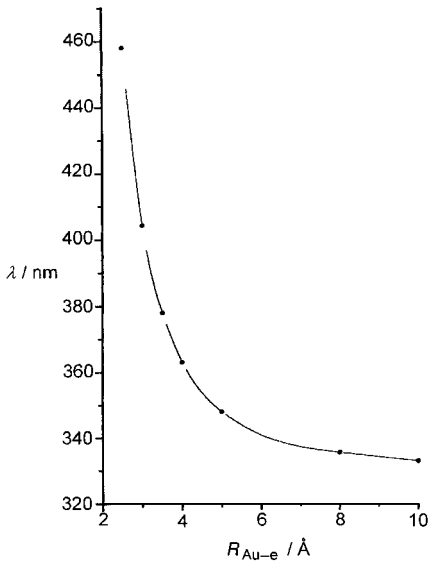

Figure 7. Plot of emission wavelength versus R_{Au-e} (distance between gold atom and background charge).

distant apart from the metal centers, and we may also expect to observe high energy emissions.

Acknowledgements

We are thankful to the Research Grants Council of the Hong Kong SAR, China [HKU 7298/99P], The University of Hong Kong, the Croucher Foundation, and the State Key Laboratory of Theoretical and Computational Chemistry of Jilin University for finanical support and the visitorship for H.-X. Z. We acknowledge Professor Vincent M. Miskowski for the helpful discussion.

[1] a) H. Schmidbaur, *Gold Bull*. **1990**, *23*, 11; b) H. Schmidbaur, *Chem. Soc. Rev.* **1995**, *24*, 391.
[2] a) P. Pyykkö, Y.-F. Zhao, *Angew. Chem.* **1991**, *103*, 622; *Angew. Chem. Int. Ed. Engl.* **1991**, *30*, 604; b) P. Pyykkö, *Chem. Rev.* **1997**, *97*, 597; c) P. Pyykkö, F. Mendizabal, *Inorg. Chem*. **1998**, *37*, 3018.
[3] Z. Su, H. Zhang, C.-M. Che, *Chem. J. Chin. Univ.* **1997**, *18*, 1171.
[4] Y. Jiang, S. Alvarez, R. Hoffmann, *Inorg. Chem*. **1985**, *24*, 749.
[5] C. King, J.-C. Wang, Md. N. I. Khan, J. P. Fackler, Jr., *Inorg. Chem*. **1989**, *28*, 2145.
[6] a) C.-M. Che, H.-L. Kwong, V. W.-W. Yam, K.-C. Cho, *J. Chem. Soc. Chem. Commun*. **1989**, 885; b) V. W.-W. Yam, T.-F. Lai, C.-M. Che, *J. Chem. Soc. Dalton Trans.* **1990**, 3747; c) C.-M. Che, H.-L. Kwong, C.-K. Poon, V. W.-W. Yam, *J. Chem. Soc. Dalton Trans.* **1990**, 3215.
[7] N. Nagasundaram, G. Roper, J. Biscoe, J. W. Chai, H. H. Patterson, N. Blom, A. Ludi, *Inorg. Chem*. **1986**, *25*, 2947.
[8] T. M. McCleskey, H. B. Gray, *Inorg. Chem*. **1992**, *31*, 1733.
[9] a) W. B. Jones, J. Yuan, R. Narayanaswamy, M. A. Young, R. C. Elder, A. E. Bruce, M. R. M. Bruce, *Inorg. Chem*. **1995**, *34*, 1996; b) P. Schwerdtfeger, A. E. Bruce, M. R. M. Bruce, *J. Am. Chem. Soc.* **1998**, *120*, 6587.
[10] J. M. Forward, D. Bohmann, J. P. Fackler, Jr., R. J. Staples, *Inorg. Chem.* **1995**, *34*, 6330.
[11] J. C. Vickery, M. M. Olmstead, E. Y. Fung, A. L. Balch, *Angew. Chem.* **1997**, *109*, 1227; *Angew. Chem. Int. Ed. Engl*. **1997**, *36*, 1179.
[12] L. H. Gade, *Angew. Chem.* **1997**, *109*, 1219; *Angew. Chem. Int. Ed. Engl*. **1997**, *36*, 1171.
[13] a) J. T. Markert, N. Blom, G. Roper, A. D. Perregaux, N. Nagasundaram, M. R. Corson, A. Ludi, J. K. Nagle, H. H. Patterson, *Chem. Phys. Lett*. **1985**, *118*, 258; b) Z. Assefa, F. DeStefano, M. A. Garepapaghi, J. H. LaCasce, Jr., S. Ouellete, M. R. Corson, J. K. Nagle, H. H. Patterson, *Inorg. Chem*. **1991**, *30*, 2868.
[14] H. Xiao, Y.-X. Weng, W.-T. Wong, T. C.-W. Mak, C.-M. Che, *J. Chem. Soc. Dalton Trans.* **1997**, 221.
[15] P. Pyykkö, J. Li, N. Runeberg, *Chem. Phys. Lett*. **1994**, *218*, 133.
[16] a) J. Li, P. Pyykkö, *Inorg. Chem*. **1993**, *32*, 2630; b) O. D. Häberlen, H. Schmidbaur, N. Rösch, *J. Am. Chem. Soc*. **1994**, *116*, 8241; c) O. D. Häberlen, N. Rösch, *J. Phys. Chem*. **1993**, *97*, 4970.
[17] a) W. Bensch, M. Prelati, W. Ludwig, *J. Chem. Soc. Chem. Commun.* **1986**, 1762; b) Md. N. I. Khan, C. King, D. D. Heinrich, J. P Fackler, Jr., L. C. Porter, *Inorg. Chem.* **1989**, *28*, 2150; c) S.-J. Shieh, D. Li, S.-M. Peng, C.-M. Che, *J. Chem. Soc. Dalton Trans.* **1993**, 195.
[18] W.-F. Fu, K.-C. Chan, V. M. Miskowski, C.-M. Che, *Angew. Chem.* **1999**, *111*, 2953; *Angew. Chem. Int. Ed.* **1999**, *381*, 2783.
[19] a) J. Kozelka, H. R. Oswald, E. Dubler, *Acta Crystallogr. Sect. C* **1986**, *42*, 1007; b) H.-R. C. Jaw, M. M. Savas, R. D. Rogers, W. R. Mason, *Inorg. Chem*. **1989**, *28*, 1028.
[20] C. Møller, M. S. Plesset, *Phys. Rev*. **1934**, *46*, 618.
[21] a) M. Head-Gordon, J. A. Pople, M. J. Frisch, *Chem. Phys. Lett*. **1988**, *153*, 503; b) M. J. Frisch, M. Head-Gordon, J. A. Pople, *Chem. Phys. Lett*. **1990**, *166*, 275; c) M. J. Frisch, M. Head-Gordon, J. A. Pople, *Chem. Phys. Lett*. **1990**, *166*, 281.
[22] a) J. B. Foresman, M. Head-Gordon, J. A. Pople, M. J. Frisch, *J. Phys. Chem.* **1992**, *96*, 135; b) K. Raghavachari, J. A. Pople, *Int. J. Quant. Chem*. **1981**, *20*, 1067.
[23] a) H. Zhang, K. Balasubramanian, *J. Chem. Phys.* **1992**, *97*, 3437; b) H. Zhang, K. Balasubramanian, *J. Chem. Phys.* **1993**, *98*, 7092.
[24] a) P. J. Hay, W. R. Wadt, *J. Chem. Phys.* **1985**, *82*, 270; b) P. J. Hay, W. R. Wadt, *J. Chem. Phys.* **1985**, *82*, 299; c) W. R. Wadt, P. J. Hay, *J. Chem. Phys.* **1985**, *82*, 284.
[25] M. J. Frisch, G. W. Trucks, H. B. Schlegel, P. M. W. Gill, B. G. Johnson, M. A. Robb, J. R. Cheeseman, T. A. Keith, G. A. Petersson, J. A. Montgomery, K. Raghavachari, M. A. Al-Laham, V. G. Zakrzewski, J. V. Ortiz, J. B. Foresman, J. Cioslowski, B. B. Stefanov, A. Nanayakkara, M. Challacombe, C. Y. Peng, P. Y. Ayala, W. Chen, M. W. Wong, J. L. Andres, E. S. Replogle, R. Gomperts, R. L. Martin, D. J. Fox, J. S.Binkley, D. J. Defrees, J. Baker, J. P. Stewart, M. Head-Gordon, C. Gonzalez, J. A. Pople, *Gaussian 94*, Rev. A.1, Gaussian Inc., Pittsburgh, PA, **1995**.
[26] J. D. Basil, H. H. Murray, J. P. Fackler, Jr., J. Tocher, A. M. Mazany, B. Trzcinska-Bancroft, H. Knachel, D. Dudis, T. J. Delord, D. O. Marler, *J. Am. Chem. Soc.* **1985**, *107*, 6908.

Received: September 14, 1998
Revised: June 18, 2001 [F1344]